

## Effect of various factors on the measurement error of structural components of machine parts materials microhardness using computer vision methods

**Abstract.** To assess the causes of failure of parts in operation, it is often necessary to assess the degradation of the structural and phase composition of the material and determine the cause of its change. Microhardness test is used to evaluate the mechanical properties of microvolumes of the material. Microhardness of structural components of steels and cast irons (armco iron ferrite, austenitic component of steel 12X18H10T and cementite of centrifugally cast chrome-nickel cast iron (cast coating Ø910 mm)) was determined by restored four-sided pyramid impression with a square base and a top angle of  $136\pm 1$ . The paper evaluates the influence of the main factors on the micro-hardness error of ferritic, austenitic and carbide component of steels and cast irons: the amount and speed of the indenter load, the stiffness of the substrate, the field of distribution of plastic deformations around the impression, the quality of the surface preparation, the influence of grain boundaries and the relaxation of the impression shape over time. The main factors affecting the accuracy of measurements by the reconstructed impression method have been determined for each of the investigated phases: ferrite, austenite, and cementite.

**Streszczenie.** Aby ocenić przyczyny awarii części w eksploatacji, często konieczna jest ocena degradacji składu strukturalnego i fazowego materiału oraz określenie przyczyny jego zmiany. Do oceny właściwości mechanicznych mikroobjętości materiału stosuje się test mirotwardości. Mirotwardość składników strukturalnych stali i żeliwa (feryt żelaza armco, austenityczny składnik stali 12X18H10T i cementyt odśrodkowo odlewanej żeliwa chromowo-niklowego (powłoka odlewu Ø910 mm)) określono przez przywrócony wycisk piramidy czterobocznej o podstawie kwadratowej i kącie wierzchołkowym  $136\pm 1$ . W pracy oceniono wpływ głównych czynników na błąd mirotwardości ferrytycznego, austenitycznego i węglkowego składnika stali i żeliwa: wielkości i prędkości obciążenia wglębnika, sztywności podłoża, pola rozkładu odkształceń plastycznych wokół wycisku, jakości przygotowania powierzchni, wpływu granic ziaren oraz relaksacji kształtu wycisku w czasie. Określono główne czynniki wpływające na dokładność pomiarów metodą zrekonstruowanego wycisku dla każdej z badanych faz: ferrytu, austenitu i cementytu. (Wpływ różnych czynników na błąd pomiaru mirotwardości materiałów elementów konstrukcyjnych części maszyn z wykorzystaniem metod wizji komputerowej)

**Keywords:** microhardness; measurement error; ferrite; austenite; cementite; load on the indenter; indentation size effect; computer vision;  
**Słowa kluczowe:** mirotwardość; błąd pomiaru; feryt; austenit; cementyt; obciążenie wglębnika; efekt wielkości wglębnienia; widzenie

### Introduction

The development of modern mechanical engineering goes hand in hand with the increase in the unit capacity of parts (operating temperatures [1], specific stresses [2], etc.). The materials of such parts, iron-carbon alloys (steels and cast irons), on the one hand, work under extreme conditions of complex temperature and force loads [3]. On the other hand, they often have a heterogeneous structure with a cross-section gradient of properties to ensure greater compliance with operational requirements [4]. Such parts must ensure guaranteed quality and reliability, including in terms of strength and durability, throughout the entire life cycle of the products. When in operation, the operating parameters of such products change over time.

As a result, individual parts and assemblies in such conditions are subjected to cyclic temperature and force effects; residual stresses are formed, which in combination with external loads can lead to local microdeformations [5], and even microcracks [6-8]. The long service life of machines also leads to a change in the structural state and trans-formation of the phase composition of materials [9], which reduces the durability of products.

Non-destructive control methods are usually used to predict the final service life of parts under extreme conditions. When parts fail in operation, it is important to assess the degree of degradation of material properties and the causes of damage. One of the common methods of evaluating the mechanical properties in microvolumes of the material is the microhardness test.

Microhardness is an indicator of the mechanical properties of microvolumes of the material [10,11] and physically represents the resistance of the material to local

de-formation when pressed, predominantly, by a pyramidal indenter [12]. The main advantage of this shape of indenters is the geometric similarity of the unrestrained impression when the amount of load changes [13, 14]. It is believed that the distribution of deformations and stresses around the impression is geometrically similar, provided that the indenter has a geometrically similar pyramidal shape in the entire range of loads [15, 16]. Such a statement may be true for materials homogenized by special processing. However, the vast majority of parts are made of materials with a heterogeneous structure [17], with a gradient of mechanical properties formed according to their operating conditions [18]. Therefore, many authors note that microhardness can depend on the load [19-21].

Currently, the measurement of microhardness by the restored imprint method of various structural components of steels and cast iron is regulated by ASTM E384-17 «Standard Test Method for Microindentation Hardness of Materials». Traditionally, for such measurement a four-sided pyramid with a square base and an angle at the top of  $136 \pm 1^\circ$  is used. The choice of such a diamond tip is based on the result of observations, according to which, when an indenter is introduced into a homogeneous material, the hardness numbers do not depend on the applied load in the range from 1 to 100 kg (from  $1 \times 10^3$  3N up to  $1 \times 10^4$  4 N). This allowed to assume that with loads of less than 1 kg ( $1 \times 10^3$  3N) the hardness values remain constant. However, the conducted studies of measuring the microhardness of ferrite, austenite and cementite [22-24] performed at various loads (0.049–1.962 N) did not confirm this assumption.

The decrease in hardness with increasing applied load is known as indentation size effect (ISE) [25, 26] and the increase in hardness with increasing applied load is known as reverse indentation size effect (RISE) [27, 28]. Some studies include image analysis of the unrestored impression, using also scanning electron microscopy to improve the accuracy of measurements [29, 30]. However, there is no data on the time that precedes the processing of the measurement and the completion of the identification process [31]. This increases the uncertainty of the microhardness and can lead to unreliable results, especially at low loads. Degradation of material properties during the operation of parts, which leads to premature failures, requires a mandatory comparison of initial and post-failure microhardness [32–35]. These data are separated in the time of measurement. Therefore, it is important to have an idea of the possible error when comparing values to find the degree of degradation of properties and causes of failures.

The aim of the work is to evaluate the effect of various factors on the measurement error of microhardness of ferritic, austenitic and carbide components of steels and cast irons. To achieve this goal, we studied the effect of the indenter loading magnitude and speed, substrate stiffness, distribution field of plastic deformations around the imprint on the level of microhardness, its spread. The effect of strip preparation quality, the effect of grain boundaries and imprints shape relaxation over time were also studied.

### Material and methods

Microhardness was evaluated on the device “Vikvant-HNADU” (patents of Ukraine No. 50486A cl.G01N 3/46 and No. 200201057) by the method of the restored imprint when introducing a diamond tip with the shape of the working part in the load range of 0.049–1.962 N (5–200 g). Arm-co-iron ferrite, austenitic component of steel 12X18N10T and cementite of centrifugal cast chromium-nickel cast iron (casting Ø910 mm) were studied.

### Results

Indenter introduction into a solid is accompanied by displacement of the material and elastic-plastic deformation of the zone adjacent to the imprint.

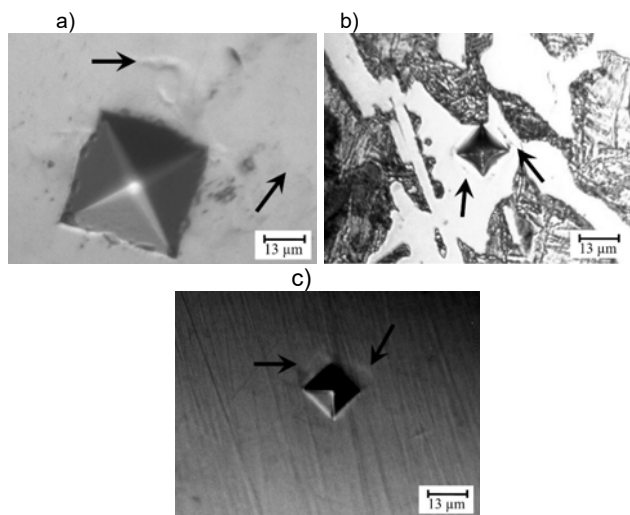


Fig. 1. Zones of Plastic Deformation of Ferrite (a), Cementite (b) Around the Imprints under a Load of 1.962 N and Austenite (c) under a Load of 0.49 N. The arrows indicate the contours of the plastic deformation zone, including at inclusions and at the grain boundary.

Deformation around the imprint is heterogeneous and covers a significant volume (Figure 1) – up to 120% for ferrite, up to 80% for austenite and up to 25% for cementite. Grain boundaries and inclusions decorate the plastic deformation zone.

When the tip is inserted, the deformations are not the same in different directions – the largest deviations are noted at the middle of the sides, and the smallest – at the corners of imprint (Figure 2, a). Etching of the surface decorates the area of maximum deformations directly at the edge of imprint (Figure 2, b). It is established that the area of plastic deformation of ferrite and austenite is heterogeneous. It consists of two zones (Table 1). The first is the zone of reduced micro-hardness (softening is 2–10% compared to the average value for the phase). This zone in the form of a dark rim along the edge of imprint is clearly visible when measuring the microhardness of ferrite on the etched surface of the strip (see Figure 2, b) and has a length of 0.5–3 microns. The second deformation zone is hardened by 5–20% and has a much larger size (7–11 times compared to the first zone). The zone of plastic deformation of cementite consists of one zone (see Table.1) – reduced microhardness. The softening zone is followed by a zone without visible de-formation.

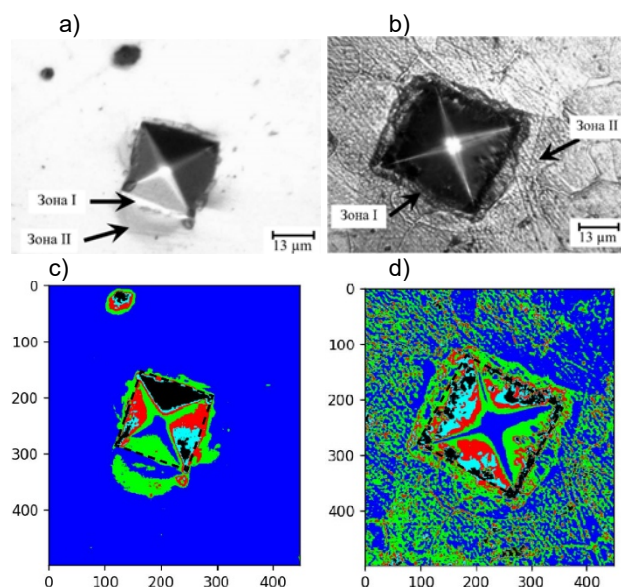


Fig. 2. Deformation Around the Imprint in Ferrite: a – before and b – after Etching with a 4% Solution of HNO<sub>3</sub>. The load corresponds to 0.49 N (a) and 1.962 N (b). Zones I and II correspond to the areas of softening and hardening of metal, respectively

Table 1. Average Microhardness of Deformation Zones Around Imprints for Different Phases.

Research Phase	In general, for the structural component	Microhardness			
		Softening Area (Zone I) Average Value	extent <sup>1</sup> , microns	Hardening Area (Zone II) Average Value	extent, microns
Ferrite	H <sub>0.196</sub> =215–220	H <sub>0.196</sub> =210–215	up to 2 µm	H <sub>0.196</sub> =220–240	up to 22 µm
Austenite	H <sub>0.196</sub> =350–360	H <sub>0.49</sub> =360–365	up to 1 µm	H <sub>0.49</sub> =370–385	up to 7–8 µm
Cementite	H <sub>0.49</sub> =1480–1570	H <sub>0.49</sub> =1420–1450	up to 2 µm	–	–

<sup>1</sup> The extent of the deformation zones was estimated by measuring microhardness and metallographic studies.

According to the requirements of GOST 9450, the distance from the center of imprint to the edge of the product must be at least double the size of the imprint. The distance between the centers of imprints applied to one surface should exceed the size of imprint by more than three times. When studying the structural components of various materials, due to the small size of austenite zones,

the presence of grain boundaries and inclusions for ferrite, increasing the dispersion of the carbide phase, it becomes necessary to perform multiple measurements closer to the recommended interval. The effect of the distance between the imprints centers on the level of fixed microhardness was studied (Figure 3), taking into account zones of plastic deformation (see Table 1).

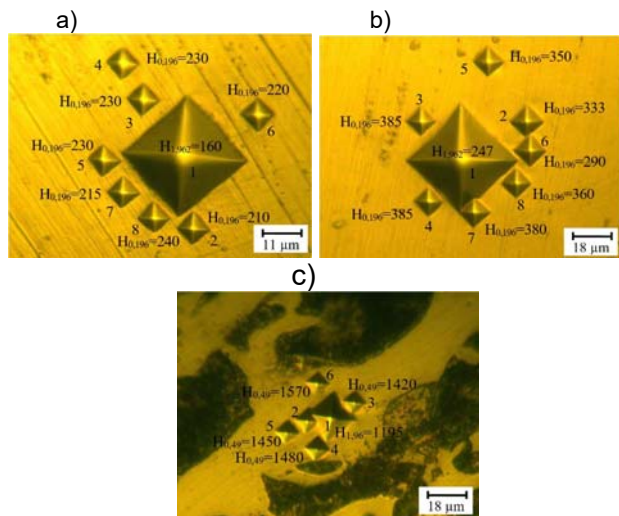


Fig. 3. Evaluation of the Distance Effect Between the Imprints on the Microhardness of Ferrite (a), Austenite (b) and Cementite (c). The order of measurements is indicated by numbers, where the load corresponds to 1.962 N and 0.196 N.

It is established that with uniform deformation of ferrite and austenite around the imprints obtained under loads in the range of 0.049 N – 1.962 N, it is necessary to take into account their orientation when assessing microhardness. Thus, when measuring ferrite at the side face of the initial imprint, the distance between the centers of subsequent imprints should exceed the diagonal size by more than 2.5 times (for austenite by 2 times), and near the corner it can be reduced up to two times (up to 1.7 times for austenite). The main feature of indenting the carbide phase is the need to select a load that would contribute less to the appearance of microcracks and chips (Figure 4). From the point of view of the imprint side shape effect, the most rational is the use of loads of 0.196 N and 0.49 N. Measurements should be made at a distance of one and a half diagonals from the side face and the corner of the imprint.

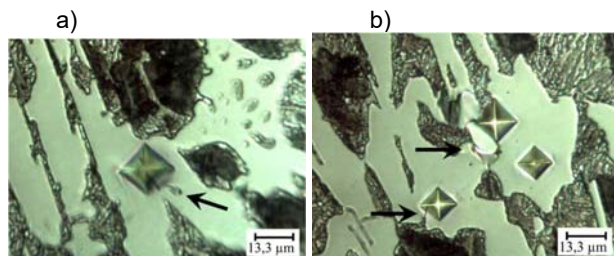


Fig. 4. Cracks under the Imprint (a), as Well as Chips and Cracks in the Carbide Phase (b) when Indenting with a Load: a – 1.962 N; b – 0.49 N.

During testing, the rate of indenter lowering is determined by the operator and affects the shape of the imprint. With its increase, a slight rotation of the indenter is observed. On imprints at a load of 1,962 N, this leads to deformation of the edges (Figure 5, a), and at low loads of

0.098 N and 0.196 N can be determined by the shape of the plastic deformation zone – there is a distinct contour characteristic of tangential stresses (Figure 5, b). Indenter rotation leads to increase in imprint diagonal, and, as a consequence, to a decrease in the microhardness value for ferrite and austenite by 3-15%. Increase in the indenter loading speed for cementite does not lead to a visible rotation and a change in imprint diagonal.

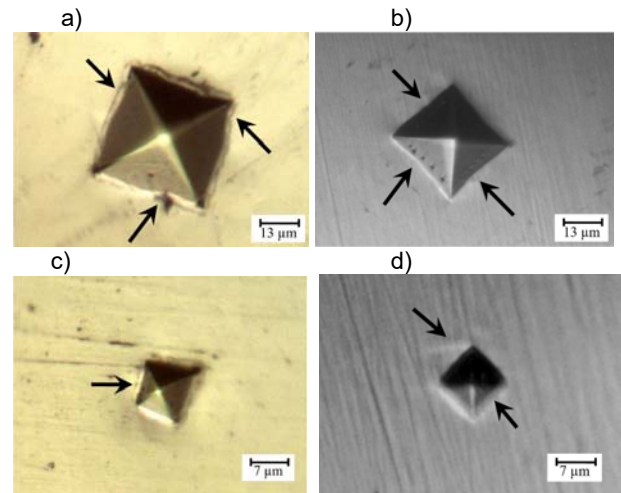


Fig. 5. Distortion of the Imprint Shape at Loads of 1.962 N for Ferrite (a) and Austenite (b), 0.49 N Ferrite (c) and 0.098 N Austenite (d). The arrows indicate the convex and concave sides of the print.

Sample inclination when it is fixed on the slide table of the device increases the microhardness values of ferrite and austenite by an average of 12-15% (see Figure 5, c). At the same time, no such changes have been recorded for cementite. The amount of fixed microhardness is also effected by the method of sample fixing. Application of a load of 1,962 N to the sample mounted directly on the slide table leads to elastic deformations of the indenter-sample-slide table system and decrease in the diagonal of the imprint. At the same time, an increase in microhardness is recorded compared to fixing on a plastic substrate by 7-10%. If the object is correctly fixed, shape of the imprint when measuring ferrite has an almost even or convex edge (Figure 6, a). Measurements at the grain boundaries change its shape to a concave one (Figure 6, b). The error introduced by the deformation of the imprint faces for ferrite at low loads (0.049 N – 0.098 N) does not exceed 3 – 5%.

$$(1) \quad H_{act} = H_{calc} / (1,8855 a/d - 0,3333),$$

where

H<sub>act</sub> is the actual microhardness,

H<sub>calc</sub> is the microhardness calculated in accordance with GOST 9450, a is the distance between the midpoints of the sides, d is the diagonal of the imprint.

Error introduced by the restored imprint sides deformation for the austenite of the steel under study is 2-3%. Shape of the imprint when measuring cementite is convex at loads of 0.049 N and 0.098 N, has an almost even edge at a load of 0.196 N and is concave at large 0.490 N – 1.962 N (Figure 6, c – d). Error introduced by the restored imprint sides deformation for maximum and minimum loads reaches 11-13%.

According to the requirements of GOST 9450, the roughness of the test surface of the sample should not be more than Ra = 0.32 microns. However, it is difficult to pro-

vide such conditions for materials containing solid non-metallic inclusions or a brittle carbide phase.

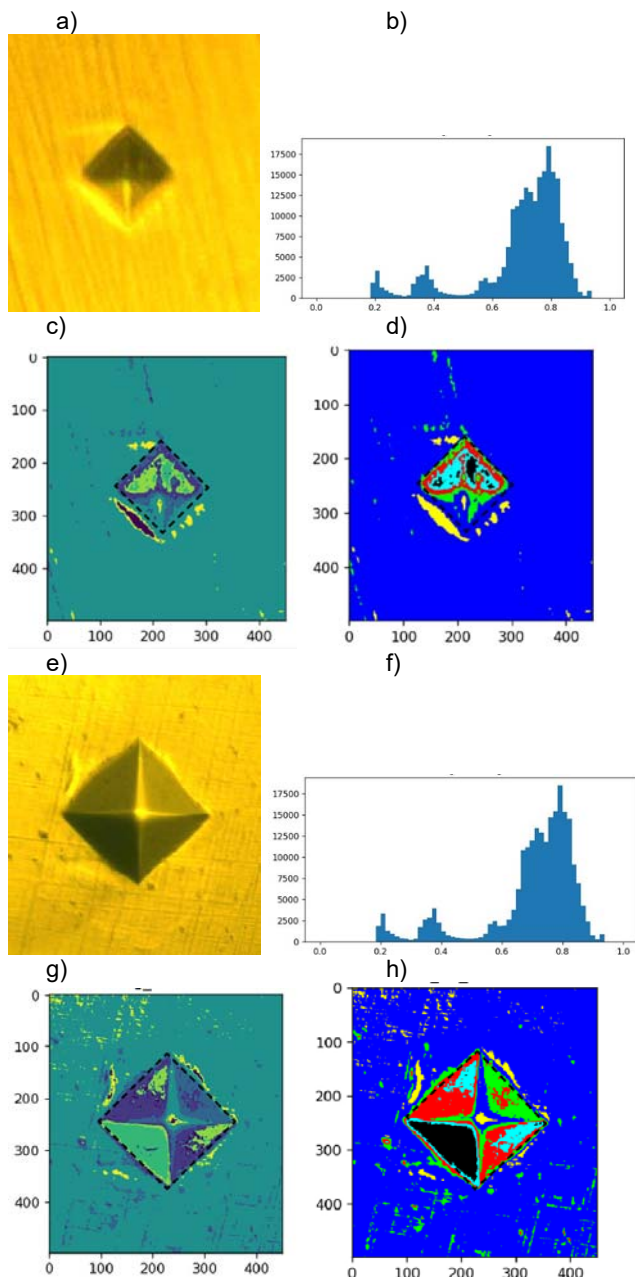


Fig. 5\_1. Illustration of the marker-based watershed segmentation workflow on a 2D image of microstructure of distortion of the Imprint Shape at Loads of 0.98 N for austenite (a) and 1.962 N for Ferrite (e) after annealed (contains all structural components). b, f – the histogram of gray values image after non-local means denoising and equalization for preserving textures; c, g - markers image after exposure (labeling 6 components of phases); d, h - the segmented image with regions resulting from the marker-based watershed segmentation (the color corresponds to the segment; yellow - zones of plastic deformity after pressing an indentant at high lowering rate; blue - matrix base (ferrite or austenite); black, red, green, azure - different zones after extracting an indentary).

It was found that at a load of 0.49 N, the presence of single scratches on the surface under the indenter increases the fixed value of microhardness by 5-12%. The presence of a large number of small scratches reduces the level of microhardness by 20 – 23%. In addition, when preparing the surface of the test sample, it is necessary, in accordance with GOST 9450, to exclude a change in the

hardness of the test surface due to riveting during machining. However, this requirement is difficult to implement, since when measuring austenite, the material hardens when the indenter is inserted into the material.

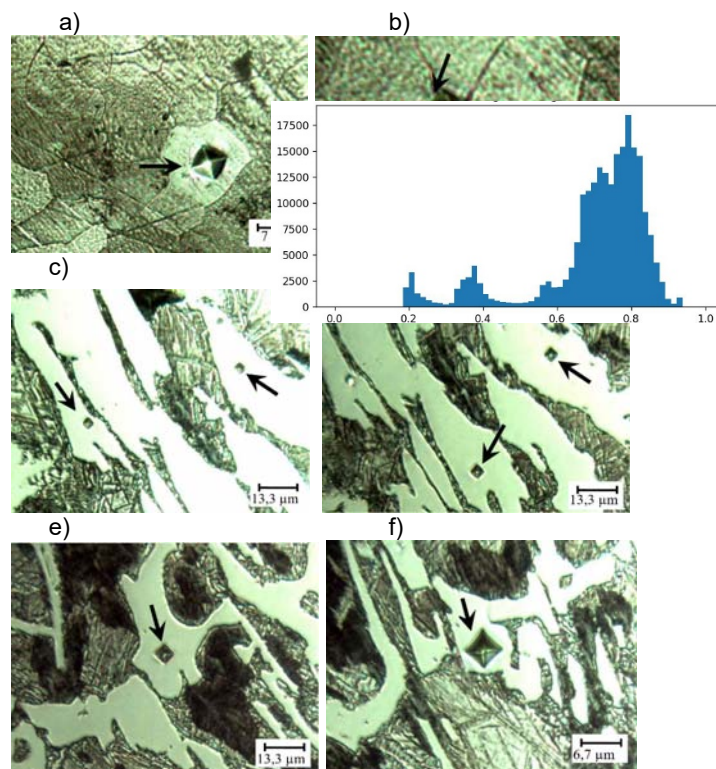


Fig. 6. Distortion of the Imprint Shape for Ferrite at Loads of 0.49 N in the Center of the Grain (a) and at the Grain Boundary (b), as well as Cementite at Loads of 0.049 N (c), 0.098 N (d) and 0.196 N (e). The arrows indicate the convex and concave sides of the print. High plasticity of the austenite of the studied 12X18H10T steel samples contributes to the formation of large zones of deformed metal with a ridge removed from the edges of the imprint and, as a consequence, the concave sides of the imprint (see Fig. 1, c). Therefore, when calculating the microhardness on the actual surface of the pyramid imprint, the curvature of the sides was taken into account according to the formula proposed by V.K. Grygorovych [5]:

According to the requirements of GOST 9450, in order to obtain the most accurate result of microhardness measuring, the load on the indenter should be as large as possible. However, our studies [2-4] have confirmed the need to justify the choice of load when different phases measuring. To assess the optimal load level when determining the microhardness of the phases, the microhardness and deviation were determined by changing the load in the range of 0.049 N – 1.962 N (Figure 7). Two samples were examined for ferrite and austenite. In the first, the studies were carried out on the non-etched surface of the grinds without taking into account the effect of grain boundaries (Figure 7, a, b, d, e). In the second sample, measurements were performed within the grains after etching the grinds surface (Figure 7, c, d, w, h). For studied samples, the presence of a dimensional effect was established, namely, a decrease in the level of microhardness with an increase in the load on the indenter from 0.196 N to 1.962 N. The data obtained are close to those given in the works of Yu.I. Golovin [6] and S.A. Fedosov and L.Peshek [9]. When measuring ferrite and austenite for small loads, a decrease in the micro-hardness level was recorded by 0.7–4.6% for 0.098 N and 35.2–50% for the minimum – 0.049 N. A decrease in the

microhardness of cementite was noted with an increase in the load on the indenter from 0.49 N to 1.962 N. For small loads, a decrease in the micro-hardness level by 47% was recorded when indenting with a load of 0.049 N compared to 0.196 N. Thus, when measuring the microhardness of cementite, a load of 0.196 N is sufficient to obtain reliable data on the properties of this phase.

Special studies have established that the effect of the ferrite grain boundary on the increase in microhardness (by 82%) is maximal when indenting with a load of 0.049 H (Figure 8). At the same time, for austenite, the effect of grain boundaries on the micro-hardness level is less significant – 10-15%.

It is established that the measurement error in this case can range from 5% to 15%. Such a large spread was obtained at the boundary permissible deviations of the inter-focal distance. A much smaller error is introduced by automatic focusing. In this case, the error does not exceed 3%.

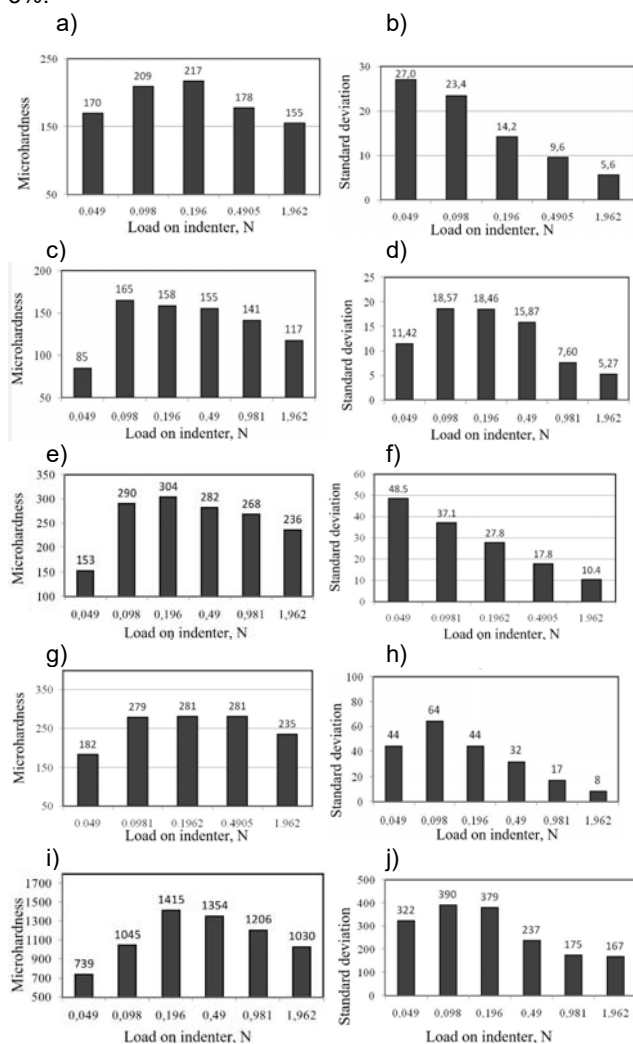


Fig. 7. Average Microhardness (a, c, e, g, i) and Standard deviation (b, d, f, h, j) of Ferrite (a – c), Austenite of Steel 12X18N10T (e – i) and Cementite of Chromium-Nickel Cast Iron (j, h) for Various Loads: a, b, e, f – Without Taking into Account Grain Boundaries; c, d, g, i – Within the Studied Phase.

To reduce the effect of random errors on the measurement result, according to GOST 9450, it is recommended to make several measurements of the same imprint (with diagonals over 10 microns – three measurements, with smaller diagonals – a larger number of measurements, taking into account the arithmetic mean of

the values obtained). However, such a recommendation requires clarification. It is established that the removal of the load when measuring the microhardness of ferrite and austenite by the method of the reconstructed imprint leads to a decrease in diagonals size, and, as a result, increase in microhardness by 10-12% is recorded after 5-20 minutes. Special studies have found that 6 months after the receipt of imprints at a load of 0.196 N and 1.962 N, the size of the diagonals decreases by 1.06–1.08 times, which corresponds to an increase in microhardness by 15-20%. The lower the load during indentation, the more imprint is restored after removing the load. When measuring the microhardness of cementite, the imprint is restored, which leads to a decrease in the diagonals size obtained during indentation in the entire studied load range of 0.049 N - 1.962 N, and, as a result, an increase in microhardness from 2 to 30% is recorded. Unlike austenite and ferrite, increase in the load during cementite indentation almost unambiguously reduces the degree of fingerprint recovery and can be estimated by dependence (with a confidence probability of 0.8):

$$(2) \Delta X = -14,03Y + 27,96,$$

where

$\Delta X$  is the degree of imprint restoration relative to the original, %;  $Y$  is the indenter load, N.

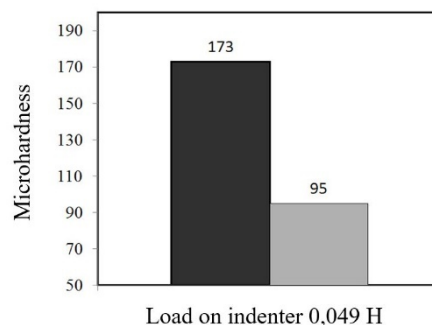


Fig. 8. Effect of the Ferrite Grain Boundary on the Increase in Microhardness during Indentation with a Load of 0.049 N: ■ - at the Grain Border, □ - in the Center of the Grain.

## Conclusion

1. It was found that the measurement error of the microhardness of ferrite is effected by: increase in the rate of indenter lowering (the microhardness value decreases by 9.5 – 12.5%); sample slope when it is fixed on the instrument base table (on average by 12-15%); imprint sides deformation at low loads of 0.049 N – 0.098 N (on 3 – 5%). Quality of the slot surface preparation (presence of single scratches under the indenter increases microhardness by 4.5 – 12%, and a large number of small scratches by 21 – 22.5%); deviations in operator camera focus, when sharpening the imprint while changing the study area, change the microhardness values by 3 – 13%, restoring the imprint size after loads removing increases microhardness by 9.5 – 11%. When measuring the microhardness of ferrite at the side face of a previously obtained imprint, the distance between the centers of subsequent imprints should exceed the diagonal size by more than 2.5 times, and near the corner it can be reduced up to two times. Grain boundaries significantly effect the level of microhardness at low loads (0.049 H) increasing it by 82%. It is recommended to measure the microhardness level of ferrite with loads of 0.098 N, 0.1962 N, at which the highest measurement accuracy is ensured.

2. It was found that with increasing load, the austenite microhardness readings become more uniform – the minimum standard deviation of 10.4 corresponds to the maximum load of 1.962 N. However, it is recommended to measure the level of austenite microhardness with smaller loads of 0.4905 N and 0.1962 N, since this ensures not only stable indicators, but also the most accurate level of it.

3. Increase in the loading speed of the indenter when measuring cementite does not lead to a visible turn and a change in imprint diagonal. Effect of sample inclination when it is fixed on device working surface on the microhardness values was also not revealed. When the tip is inserted, the deformations (14-23% in extent) are not the same in the same directions as austenite, ferrite - the largest deviations are noted at the middle of the sides, and the smallest - at the corners of the imprint. Error introduced by re-stored imprint sides deformation for maximum and minimum loads (0.49 N – 1.962 N) reaches 11-13%. Measurements of the microhardness of cementite should be made at a distance of one and a half diagonals from the side face and the corner of the imprint. At the same time, the recommended load, which provides the highest measurement accuracy, is 0.1962 N.

### Acknowledgement

Funded by a subsidy of the Ministry of Education and Science for the Agricultural University of Hugo Koffajtaj in Krakow for 2022.

**Authors:** Vitaliy Vlasovets, Department of tractors and cars, State Biotechnology University, Alchevsky St., 44, Kharkiv, 61002, Ukraine; E-mail: vlasovets@ukr.net; Tatiana Vlasenko, Department of tractors and cars, State Biotechnology University, Alchevsky St., 44, Kharkiv, 61002, Ukraine; Stepan Kovalyshyn Professor, Lviv National Agrarian University, Vol. Velykogo str., 1, 80381 Dubliany, Ukraine E-mail: stkovalyshyn@gmail.com; Olesy Kovalyshyn, Department of cars and tractors, Lviv National Agrarian University, V.Valyki Street, 1, Dubliany, 80381, Ukraine; Oleg Kovalyshyn, Soft Serve Digital Consulting Company, Lviv, Ukraine, Sławomir Kurpaska, Professor University of Agriculture in Krakow, Faculty of Production and Power Engineering, Balicka Av. 116B, 30-149 Krakow, E-mail:slawomir.kurpaska@urk.edu.pl; Paweł Kielbasa Associate Professor, University of Agriculture in Krakow, Faculty of Production and Power Engineering, Balicka Av. 116B, 30-149 Krakow, E-mail:pawel.kielbasa@urk.edu.pl; Oleksandra Bilovod, Department of Industry Engineering, Poltava State Agrarian University, St. Skovoroda 1/3, Poltava,36003, Ukraine, Lyudmila Shulga, Department of Industry Engineering, Poltava State Agrarian University, St. Skovoroda 1/3, Poltava,36003, Ukraine

### REFERENCES

- [1] Kurpaska, S.; Latała, H.; Kielbasa, P.; Sporysz, M.; Gliniak, M.; Famielec, S.; Bogusława. Experimental and modeling approach to heat and mass transfer in a porous bed of a rock-bed heat accumulator. *International Journal of Heat and Mass Transfer* 2021, Volume 132, 179.
- [2] Hu, Y., Wu, S., Withers, P.J., Cao, H., Chen, P., Zhang, Y., Shen, Z., Vojtek, T., Hutař, P. Corrosion fatigue lifetime assessment of high-speed railway axle EA4T steel with artificial scratch. *Engineering Fracture Mechanics* 2021, Volume 245, 107588.
- [3] Jafari, D., Vaneker, T.H.J., Gibson, I. Wire and arc additive manufacturing: Opportunities and challenges to control the quality and accuracy of manufactured parts. *Materials and Design* 2021, Volume 202, 109471.
- [4] Meng, L., Zhu, B., Xian, C., Zeng, X., Hu, Q., Wang, D. Comparison on the wear properties and rolling contact fatigue damage behaviors of rails by laser cladding and laser-induction hybrid cladding. *Wear* 2020, Volume 458-459, 203421.
- [5] Sun, Q., Zhou, J., Li, P. Simulations and Experiments on the Micro-Milling Process of a Thin-Walled Structure of Al6061-T6. *Materials* 2022, Volume 15(10), 3568
- [6] Efremenko, B.V., Chabak, Y.G., Efremenko, V.G., Vlasovets, V.M. Kinetics of structure transformation in pulsed plasma high-Cr coatings under post-heat treatment. *Functional Materials* 2020, Volume 27(1), pp. 117-124.
- [7] Pawłowski, S.; Plewako, J.; Korzeniewska, E. Influence of Structural Defects on the Resistivity and Current Flow Field in Conductive Thin Layers. *Electronics* 2020, 9, 2164. <https://doi.org/10.3390/electronics9122164>
- [8] Pawłowski, S.; Plewako, J.; Korzeniewska, E. Influence of the geometry of defects in textronic structures on their electrical properties; *Journal of Physics: Conference Series*, Volume 1782, 2020 Applications of Electromagnetics in Modern Engineering and Medicine (PTZE 2020) 13-16 September 2020, virtual meeting, Poland; 012027
- [9] Kovalyshyn, S., Kharchenko, S., Borshch, Y., Piven, M., Abduev, M., Miernik, A., Popardowski, E., Kielbasa, P. Modeling of aerodynamic separation of preliminarily stratified grain mixture in vertical pneumatic separation duct. *Applied Sciences (Switzerland)* 2021, Volume 11(10).
- [10] Cantor, B., Chang, I.T.H., Knight, P., Vincent, A.J.B. Microstructural development in equiatomic multicomponent alloys. *Materials Science and Engineering* 2004, A, Volume 375-377(1-2 SPEC. ISS.), pp. 213-218.
- [11] Yangfan, W., Xizhang, C., Chuanchu, S. Microstructure and mechanical properties of Inconel 625 fabricated by wire-arc additive manufacturing. *Surface and Coatings Technology* 2019, Volume 374, pp. 116-123.
- [12] ASTM E384-17 «Standard Test Method for Microindentation Hardness of Materials»
- [13] Van Der Voort, G.F. Avoid Microindentation Hardness testing at low loads! *ASTM Special Technical Publication* 2019, pp. 66-73.
- [14] Petřík, J., Blaško, P., Mihalíková, M., Vasilňáková, A., Mikloš, V. The relationship between the deformation and the indentation size effect (ISE). *Metallurgical Research and Technology* 2019, Volume 116(6).
- [15] Petřík, J., Blaško, P., Mikloš, V., Pribulová, A., Futaš, P., Vasilňáková, A., Šolc, M. The load dependence of the microhardness of the blast furnace slag. *Metallurgical and Materials Engineering* 2020, Volume 26(3), pp. 329-340.
- [16] Blaško, P., Kupková, M., Petrik, J., Futaš, P., Vasilňáková, A. The indentation size effect of sintered Fe/3.3 wt-%Cu + CnHm measured by Vickers scale. *Materials Science and Technology (United Kingdom)* 2020, Volume 36(4), pp. 403-408.
- [17] Pastrňák, M., Hilšer, O., Ruzš, S., Reška, V., Szkauder, P., Zabyszczan, R. Effect of processing route on microstructure and microhardness of low-carbon steel subjected to drece process, *Metal 2021 - 30th Anniversary International Conference on Metal-lurgy and Materials*, Conference Proceedings 2021, pp. 323-328.
- [18] Karthick, K., Malavizhi, S., Balasubramanian, V. Microstructural characterization of dissimilar weld joint between ferritic steel and stainless steel. *Materials Science and Technology (United Kingdom)* 2021, 37(15), pp. 1257-1269.
- [19] Papadopoulou, S., Pressas, I., Vazdirvanidis, A., Pantazopoulos, G. Fatigue failure analysis of roll steel pins from a chain assembly: Fracture mechanism and numerical modeling. *Engineering Failure Analysis* 2019, 101, pp. 320-328.
- [20] Petřík, J. On the Load Dependence of Micro-Hardness Measurements: Analysis of Data by Different Models and Evaluation of Measurement Errors. *Archives of Metallurgy and Materials* 2016, Volume 61(4), pp. 1819-1824.
- [21] Petřík, J., Palfy, P. The influence of the load on the hardness. *Metrology and Measurement Systems* 2011, 18(2), pp. 5.
- [22] Saha, D.C., Biro, E., Gerlich, A.P., Zhou, Y. Martensite tempering kinetics: Effects of dislocation density and heating rates. *Materials Characterization* 2020, 168.
- [23] Baharvand, M., Zanganeh, A., Mirzadeh, H., Habibi Parsa, M. Effects of hot rolling and homogenisation treatment on low alloy steel ingot. *Materials Science and Technology (United Kingdom)* 2020, 36(7), pp. 835-842.
- [24] Tong, Z., Liu, H., Jiao, J., Zhou, W., Yang, Y., Ren, X. Microstructure, microhardness and residual stress of laser additive manufactured CoCrFeMnNi high-entropy alloy subjected to laser shock peening. *Journal of Materials Processing Technology* 2020, 285.
- [25] Petřík, J., Blaško, P., Markulík, Š., Šolc, M., Palfy, P. The Indentation Size Effect (ISE) of Metals. *Crystals* 2022, 12(6).

- [26] XU, Z., PENG, L., BAO, E.. Size effect affected springback in micro/meso scale bending process: Experiments and numerical modeling. *Journal of Materials Processing Technology* 2018, 252, pp. 407-420.
- [27] Bhattacharya, S., Kundu, R., Bhattacharya, K., Poddar, A., Roy, D. Micromechanical hardness study and the effect of reverse indentation size on heat-treated silver doped zinc-molybdate glass nanocomposites. *Journal of Alloys and Compounds* 2019, 770, pp. 136-142
- [28] Sangwal, K. On the reverse indentation size effect and microhardness measurement of solids. *Materials Chemistry and Physics* 2000, 63(2), pp. 145-152.
- [29] Shilin, C., Wei, S. An algorithm for indentation image classification and detection based on deep learning. *Measurement: Sensors* 2021, 18.
- [30] Chaanthini, M.K., Arul, S. Effect of surface modification using gtaw as heat source and cryogenic treatment on the surface hardness and its prediction using artificial neural network. *Lecture Notes in Mechanical Engineering* 2018, Volume PartF7, Pages 185
- [31] Rajarajan, C., Sivaraj, P., Sonar, T., Raja, S., Mathiazhagan, N. Investigation on microstructural features and tensile shear fracture properties of resistance spot welded advanced high strength dual phase steel sheets in lap joint configuration for au-tomotive frame applications. *Journal of the Mechanical Behavior of Materials* 2022, 31(1), pp. 52-63.
- [32] Globa, S., Simmons, T., Navarro, D., Aranda, M., Ravi, V.A. Effect of austenite stability in pack aluminizing of stainless steels. *NACE - International Corrosion Conference Series* 2018, Volume 2018
- [33] Aucott, B. Current trends in metal analysis. *Foundry Trade Journal* 2004, 178(3614), pp. 154-155.
- [34] Kharchenko, S., Borshch, Y., Kovalyshyn, S., Piven, M., Abduev, M., Miernik, A., Popardowski, E., Kielbasa, P. Modeling of aerodynamic separation of preliminarily stratified grain mixture in vertical pneumatic separation duct (2021) *Applied Sciences (Switzerland)*, 11 (10), art. no. 4383.
- [35] Oziembłowski, M., Nawirska-Olszańska, A., Maksimowski, D., Trenka, M., Break, A., Kulig, D., Miernik, A. The effect of concentrated microwave field (Cmf) on selected physical and rheological properties of liquid egg products (2021) *Applied Sciences (Switzerland)*, 11 (4), art. no. 1832, pp. 1-19.